An Experimental Study of the Dynamics of the Reaction H + CO_2 → OH(v', j', f) + CO: Product State-Resolved Differential Cross Sections and Translational Energy Release Distributions

M. Brouard,* D. W. Hughes, K. S. Kalogerakis, and J. P. Simons*

The Physical and Theoretical Chemistry Laboratory, University of Oxford, South Parks Road, Oxford, OX1 3QZ, U.K.

Received: May 6, 1998; In Final Form: July 22, 1998

Angular distributions and pair-correlated translational energy distributions have been measured for OH($v' = 0$, $N' = 1$), produced through the reactive scattering of hot H atoms by CO_2 at 300 K and mean collision energies of 1.8 eV and 2.5 eV. The new measurements, together with those reported previously for the OH($v' = 0$, $N' = 5$, A'/A'') products of the reaction at 2.5 eV, reveal that the differential cross sections depend strongly on collision energy and product quantum state. For the OH($v' = 0$, $N' = 1$) channel, the angular distribution changes from broad forward scattering to pronounced backward scattering as the collision energy is raised from 1.8 to 2.5 eV. The angular distributions at the higher collision energy shift from being backward to nearly isotropic, with forward−backward peaks, as the OH angular momentum is increased from $N' = 1$ to $N' = 5$. Although somewhat less dramatic changes are evident in the pair-correlated kinetic energy release data, the measurements confirm that the CO internal energy distributions are considerably colder than those predicted by statistical phase space theory. The results are discussed in light of earlier theoretical and experimental studies, particularly the results of femtochemical kinetic measurements.

1. Introduction

There is a vast experimental and theoretical literature[1,2] relating to the kinetics and dynamics of the important combustion and atmospheric chemical reaction

$$OH + CO \rightarrow HOCO \rightarrow H + CO_2$$

The role of HOCO as a quasibound reaction intermediate is firmly established,[1,2] but many uncertainties remain regarding the dynamics of its unimolecular decomposition as well as the possible role of HCO_2 configurations at elevated collision energies, particularly those necessarily employed in photoinitiated studies of the endothermic reaction

$$H + CO_2 \rightarrow OH(v', N', f) + CO \qquad \Delta_r H_0^{\ominus} = 102 \text{ kJ mol}^{-1} \tag{1}$$

Direct measurements by the Wittig group[3,4] of the rates of unimolecular decomposition of HOCO (generated within a van der Waals complex) to OH($v' = 0$, $\langle N \rangle \sim 10$) + CO indicated lifetimes, $\tau(E)$, in the range 0.1−1.0 ps for excess energies, E, in the range 40−100 kJ mol^{-1} (measured with respect to the zero-point level at the OH + CO asymptote). Remarkably, these were in close agreement with RRKM lifetime estimates, which might be taken to indicate very fast intramolecular vibrational redistribution (IVR); the agreement should be qualified, however, by concerns regarding the "effective" value of E in the complex and uncertainties about its well depth,[5] rotational angular momentum, J, and density of states, $\rho(E, J)$.[1] Further concerns relate to an apparent dependence of the lifetime on the quantum state of the probed OH($v' = 0$, N'). An earlier "real-time" measurement,[6] conducted with laser pulses of picosecond duration, indicated a longer delay for dissociation into OH($v' = 0$, $N' = 1$) than ($v' = 0$, $N' = 6$), while the later measurements,[3,4] conducted with pulses of femtosecond duration with a frequency spread which probed *all* levels in OH($v' = 0$, $N' = 2-20$), indicated decay times one order of magnitude shorter than those measured into OH($v' = 0$, $N' = 1$). Assuming that all product channels, N', are generated by the same dissociation mechanism for the complex, these results are inconsistent with rapid IVR during the lifetime of the excited molecule.

Additionally, measurements of the internal energy distribution among the CO molecules[7] and of the state-averaged[8−10] or product pair-correlated translational energy distributions[10,11] all indicate internal energy distributions in the scattered CO molecules that are much "colder" than those predicted by phase space theoretical calculations. Better agreement can be obtained via quasiclassical trajectory (QCT) calculations[12] on a modified version of the semiempirical potential energy surface originally developed by Schatz, Fitzcharles and Harding.[13] The principle modifications included a "tightening" of the HO···CO transition state and a slight lowering of the surface corresponding to reaction via HCO_2 collision geometries. Quantum calculations (in reduced dimensions) have also predicted a long series of Feshbach resonances in HOCO, with lifetimes (widths) lying in the range 0.1−1.0 ps, continuing to energies >40 kJ mol^{-1} above the HO + CO dissociation limit.[14−16] The lifetimes obtained from these reduced dimensionality quantum mechanical (QM) calculations are broadly consistent with the results from the full dimensionality QCT calculations.

The scattered product angle-velocity distribution provides another dynamical indicator, as well as a (albeit indirect) means of estimating the average lifetime of the intermediate collision complexes. In these experiments, the "clock rate" is determined by the rotational period of the complex the two key time scales are those for IVR within the complex and for its eventual

10.1021/jp982148z CCC: $15.00
Published on Web 09/22/1998

dissociation (which are reflected in the product translational energy and quantum state distributions and the shape(s) of the angular distribution(s)). A globally averaged differential cross section (DCS) for the exothermic *reverse* reaction, determined under cross-beam conditions by Casavecchia and co-workers[17,18] at a collision energy of ~60 kJ mol^{-1}, was moderately biased in favor of forward scattering (of CO_2 with respect to OH); this was interpreted in terms of an average lifetime, $\tau(E)$, comparable to the mean rotational period of the complex, τ_R, estimated to be ~0.6 ps. A subsequent measurement by our own group[11] of the *product state-resolved* DCS for OH($v' = 0$, $N' = 5$) produced through the endothermic reaction 1 gave, remarkably, almost the identical result, although the collision energy (referenced to OH + CO) was some 90 kJ mol^{-1} higher. At these energies, the complex lifetime, $\tau(E) \ll 0.6$ ps, was expected to be much shorter than the rotational period τ_R. In addition, the pair-correlated translational energy distribution was peaked well above a phase space theoretical prediction, possibly consistent with incomplete IVR during the brief lifetime of the collision complex. The appearance of both forward and backward scattering in the DCS was taken to reflect dynamical constraints rather than rotational averaging.

The present paper explores this interpretation through a series of new measurements of the product state-resolved angular distributions and pair-correlated translational energy distributions for reaction 1. New data are presented for the scattering of OH into ($v' = 0$, $N' = 1$) at mean collision energies of 1.8 and 2.5 eV, ~70 and 140 kJ mol^{-1} above the zero-point level of the OH + CO asymptote, the former being close to the collision energy employed in the cross-beam study of the *reverse* reaction. Sections 2 and 3 outline the experimental method and summarize the procedures employed to analyze the experimental data; the results and their discussion are presented in section 4, where they are compared with the earlier data for OH($v' = 0$, $N' = 5$) determined at a collision energy of 2.5 eV. The interim conclusions and some future pointers are presented in section 5.

2. Experimental Section

The experimental procedures, which follow those described in some detail earlier,[11] are only outlined here. The reagent gases, HBr or HCl and CO_2, in a ratio of 1:5, were flowed through the reaction chamber at a total pressure of 13.3 Pa. Reaction was initiated through photodissociation of the HCl or HBr precursor, using polarized radiation at 193 nm from an ArF excimer laser. The OH(v', N', f) fragments scattered from the subsequent collision of the "hot" H atoms (providing mean collision energies of 1.8 eV (HCl) or 2.5 eV (HBr)) with the 300 K CO_2 "target" molecules were detected after a delay of 80 ns, using a tunable, line-narrowed, polarized, and frequency-doubled dye laser to excite fluorescence via absorption into individually resolved spectral features in the $\Delta v = 0$ sequence of the A ← X system.

Doppler-resolved rotational line contours for OH($v' = 0$, $N' = 1$) were recorded on either the $P_{12}(1)\uparrow$ or $R_{22}(1)\uparrow$ transitions in coaxial (case A or B) and perpendicular geometries (case D).[19] To ensure the absence of distortions associated with saturation, the linearity of the laser-induced fluorescence signal with respect to the laser intensity was regularly monitored and the laser powers were kept within this regime. The absence of collisional relaxation was ensured by controlling the total pressure and maintaining an optimum probe delay time. In contrast, the bandwidth of the probe laser was determined by recording Doppler profiles of the scattered OH under fully relaxed conditions: typically ~13 μs delay at a total pressure of ~26 Pa. After deconvolution for thermal broadening at 300 K, the full width at half-maximum for the frequency-doubled etalon-narrowed laser radiation was determined to be 0.10 ± 0.015 cm^{-1}.

3. Analytical Procedures

Linear combinations of Doppler-resolved contours, obtained using the alternative pump−probe configurations, were employed to construct two *composite Doppler profiles*,[11] which depend solely on specific moments of the laboratory (LAB) frame velocity distribution. The two composite profiles which are of relevance to the study of rotationless OH($v' = 0$, $N' = 1$) products are (i) that dependent on the OH LAB speed distribution[20]

$$D_0^0(0, 0; v_p) = \int_{v=v_p}^{\infty} \frac{1}{2v} \overline{\beta_0^0}(0, 0; v)\, P_0\left(\frac{v_p}{v}\right) dv \qquad (2)$$

and that dependent on the OH LAB translational anisotropy

$$D_0^2(2, 0; v_p) = \int_{v=v_p}^{\infty} \frac{1}{2v} \overline{\beta_0^2}(2, 0; v)\, P_2\left(\frac{v_p}{v}\right) dv \qquad (3)$$

In both equations, the profiles have been expressed in terms of the OH LAB speed, v, and the component of the OH LAB velocity, v, along the propagation axis of the probe laser, v_p, which is proportional to frequency shift. The $P_{k_1}(...)$ are the Legendre polynomials. The $\beta_0^{k_1}(k_1, 0; v)$ term represents rescaled LAB frame bipolar moments[20,11] averaged over the full spread of atomic and molecular reagent velocities. These bipolar moments may be expressed directly in terms of the OH center-of-mass (CM) angular and kinetic energy release distributions of interest.[20]

The CM frame joint probability density function $P(\sigma_t, w) \equiv (2\pi\, d^2\sigma)/(\sigma\, d\omega_t\, dw)$ for obtaining OH radicals at a CM scattering angle, θ_t, and CM speed, w, can be written in terms of a double Legendre moment expansion in scattering angle and the fraction of available energy released into translation, f_t [21]

$$P(\theta_t, w) \equiv P(\theta_t, f_t)|df_t/dw|$$

$$= {}^1/_4 \sum_{n,m} a_{nm} P_n(\cos\theta_t)\, P_m(f'_t)\, |df'_t/dw| \qquad (4)$$

where

$$f'_t = (2f_t - 1)$$

$$\left|\frac{df'_t}{dw}\right| = 2M \frac{m_{OH}}{m_{CO}} \frac{w}{E'_{t,max}}$$

and $E'_{t,max}$, the maximum possible kinetic energy release, is given by

$$E'_{t,max} = \Delta_r H_0^{\ominus} + E_t + E_{CO_2} - E_{OH}$$

M in these equations is the total mass, and E_{CO_2} and E_{OH}, appearing in the final expression, are the average internal energy of the thermal CO_2 target molecules and the *fixed* internal energy of the probed OH level, respectively. Note that f_t ($\equiv E'_t/E'_{t,max}$) is the fraction of the energy available to the particular probed OH(v', j') product which is released into translation. The analysis assumed the moments of the CM distribution to be

independent of the comparatively narrow spread of reactant relative speeds, k.

The moments of the CM distribution were extracted from the composite Doppler profiles by expressing the experimental contours as expansions in sets of basis functions,

$$D_0^{k_1}(k_1, 0; v_p) = \sum_{n,m} a_{nm} G_0^{k_1}(k_1, 0; v_p; n, m) \qquad (5)$$

with the expansion coefficients determined by simultaneous least-squares fitting to the two experimental composite profiles identified above. Each (n, m) Legendre polynomial basis function was obtained by simulating Doppler contours setting the appropriate a_{nm} Legendre moment in eq 4 to unity and the others to zero. The basis functions accommodated the full, three-dimensional spread of reagent velocities[20,11] and included the effects arising in the photon initiation step from the population of both spin−orbit states of the halogen atom with different translational anisotropies.[22] They also took account of the excitation function for the H + CO_2 reaction, determined experimentally by Wittig and co-workers,[23] and the laser line shape function. The analysis generated the Legendre moments of the joint $P(\theta_t, f_t)$ distribution, which on integration over f_t yielded the (conventional) angular distribution

$$\frac{2\pi}{\sigma}\frac{d\sigma}{d\omega_t} \equiv \frac{1}{\sigma}\frac{d\sigma}{d\cos\theta_t} = \frac{1}{2}\sum_n a_{n0} P_n(\cos\theta_t) \qquad (6)$$

and on integration over scattering angle yielded the $P(f_t)$ distribution

$$P(f_t) = \sum_m a_{0m} P_m(f'_t) \qquad (7)$$

In practice, satisfactory fits to the data could be obtained assuming a joint distribution of separable form

$$P(\theta_t, f_t) = P(\theta_t)\, P(f_t) \qquad (8)$$

for which the a_{nm} coefficients may be set equal to $a_n \times b_m$ ($\equiv a_{n0} \times a_{0m}$). Importantly, the *average* angular and $P(f_t)$ distributions derived from fits which *did not* assume separability were found to be the same as those which assumed separability, within the combined errors of the analyses. Further details about the determination of the CM distributions, together with a discussion of the Monte Carlo error analysis procedures employed,[24] will be given elsewhere.[25]

4. Results and Discussion

Figures 1 and 2 show the experimental composite Doppler profiles for the OH($v' = 0$, $N' = 1$) reaction products at the two collision energies, 1.8 and 2.5 eV. The signal-to-noise ratios on the speed dependent composite profiles are excellent. The quality of the anisotropy dependent profiles (the bottom panels of Figures 1 and 2) is less good, but this a consequence of the very low LAB frame OH translational anisotropies observed for the OH($v' = 0$, $N' = 1$) products of reaction 1 at these collision energies. These low anisotropies reflect the combined effects of the scattering dynamics and the kinematics and energetics of the state-resolved reaction.[11] The plots also show the fits and residuals obtained using the procedures described in section 3. For the lower collision energy data, which has slightly poorer signal-to-noise ratios, three moments in both cos θ_t and f_t were employed, while fits to the higher collision energy data were obtained with four moments in scattering angle and three in f_t. The truncation of the expansion given in eq 5 was determined by the point at which negligible reduction in χ^2 for the fit occurred upon increasing the parameter space. For both sets of data, the qualitative features of the CM distributions of interest (see below) were insensitive to inclusion of higher expansion moments.

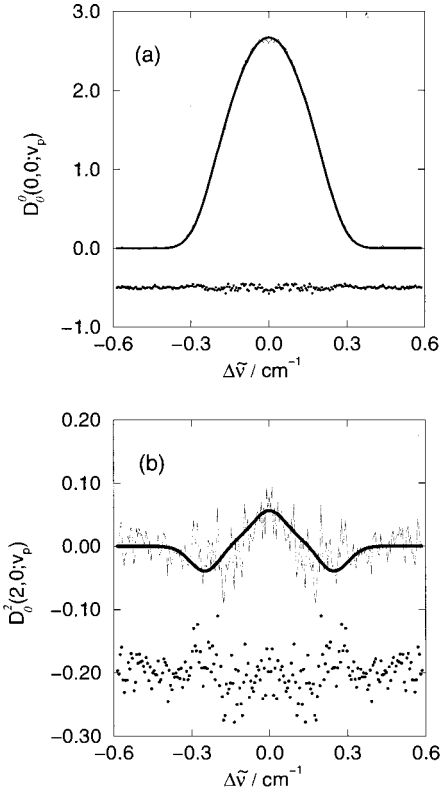

Figure 1. Doppler-resolved speed (a) and translational anisotropy dependent (b) composite Doppler profiles of the OH($^2\Pi_{1/2}$, $v' = 0$, $N' = 1$) products of the H + CO_2 reaction at a most probable CM collision energy of 1.8 eV. The smooth dark lines are the fits to the data using the procedures outlined in section 3. The experimental data are shown as a thin light line, and the offset residuals are plotted as circles at the bottom of each profile.

The angular distributions and fractional kinetic energy release distributions ($P(f_t)$) obtained at the two collision energies are shown in Figures 3 (1.8 eV) and 4 (2.5 eV). The error bars represent two standard deviations from the mean. Within these errors, the OH($v' = 0$, $N' = 1$) products at a collision energy of 1.8 eV are scattered over a wide range of angles primarily into the forward hemisphere (with respect to the incoming H atoms), while the higher collision energy data display pronounced scattering into the backward hemisphere. The kinetic energy release data also show variations with collision energy, but the most striking feature of both data sets is the fact that the $P(f_t)$ distributions peak at much higher kinetic energy releases than predicted on the basis of phase space theory (see Figures 3 and 4) [1]. (The phase space theoretical population distributions were calculated using a maximum orbital angular momentum L_{max} ~ 100 $\hbar$, but were found insensitive to L_{max} in range ~10−100 $\hbar$). Since $f_t = 1 - f_{int}^{CO}$ (where f_{int}^{CO} is the fraction of the energy available for the CO coproducts of OH($v' = 0$, $N' = 1$) which is released into CO internal excitation), the data reveal that the pair-correlated CO *internal* energy distributions at both collision energies are considerably *colder* than phase space theory prediction, a conclusion which is in general accord with the (OH state-averaged, global) CO internal state populations determined by Rice and Baronavski.[7] The results are also consistent with our previous measurements of the internal energy

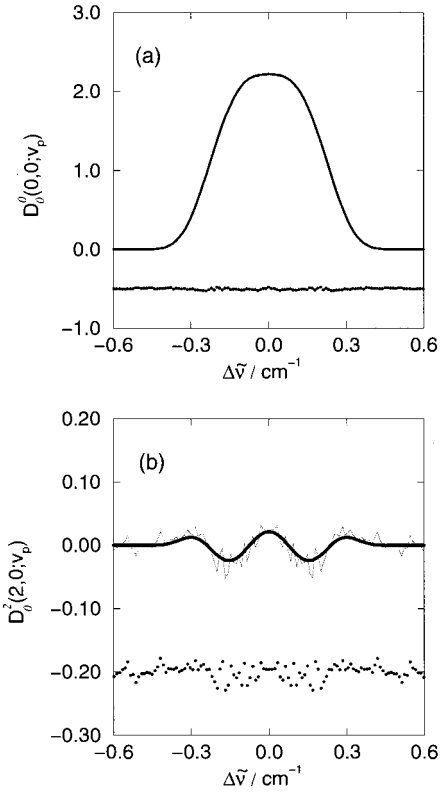

Figure 2. Doppler resolved speed (a) and translational anisotropy dependent (b) composite Doppler profiles of the OH($^2\Pi_{1/2}$, $v' = 0$, $N' = 1$) products of the H + CO_2 reaction at a most probable collision energy of 2.5 eV. The smooth dark lines are the fits to the data using the procedures outlined in section 3. The experimental data are shown as a thin light line, and the offset residuals are plotted as circles at the bottom of each profile.

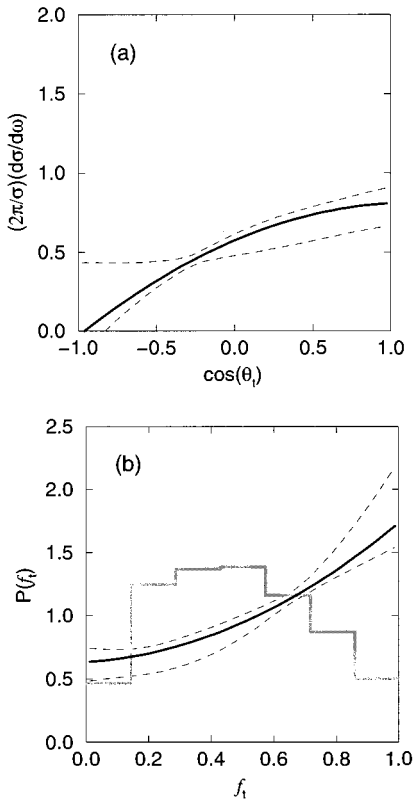

Figure 3. The OH($v' = 0$, $N' = 1$) angular distribution (a) and the distribution in the fractional energy release into translation $P(f_t)$ (b) from the H + CO_2 reaction at a collision energy of 1.8 eV. The center-of-mass scattering angle θ_t in the upper panel is that between the CM velocities of OH and the reactant H atom. The best fit results are shown as bold lines, while the 95% confidence limits, based on a Monte Carlo error analysis, are shown as dashed lines. Also shown in the lower panel as a thick gray line is the phase space predicted $P(f_t)$ distribution.

distribution of the CO coproducts of OH($v' = 0$, $N' = 5$, A'/A''), generated via reaction 1 at 2.5 eV.[11]

The dramatic variations in state-resolved scattering dynamics with increasing collision energy are summarized in the form of polar plots of the joint $P(\theta_t, w)$ distribution (see Figure 5). The data have been convoluted to account for the modest spread in reactant relative speed, k, induced by thermal motions in the precursor (HCl/HBr) and target (CO_2) molecules. The new OH($v' = 0$, $N' = 1$) results are compared in the figure with those for OH($v' = 0$, $N' = 5$, A') from our previous study of reaction 1 at a collision energy of 2.5 eV.[11] Note the OH($v' = 0$, $N' = 5$, A') state-resolved *angular* distribution[11] is nearly isotropic, with peaks in both forward and backward directions, in marked contrast to the angular distribution of OH($v' = 0$, $N' = 1$) at the same collision energy (2.5 eV). We note that our previous study found the OH($v' = 0$, $N' = 5$) angular distribution to be *in*sensitive to OH Λ-doublet level.[11]

Although quantitative interpretation of the results summarized in Figure 5 must await OH *state-resolved* QCT or QM calculations, it is tempting to speculate on the origins of the collision energy and OH quantum state dependent scattering. The measured angular distributions probe most sensitively the *relative* time scales for complex rotation and dissociation, both of which are likely to depend on total energy and (total and OH product) angular momentum. In this context, the OH($v' = 0$, $N' = 1$) angular distribution at 2.5 eV appears most readily interpretable in terms of low impact parameter, near collinear reactive collisions, leading to the formation of state-specific products on time scales much shorter than the rotational period of the collision complex. On the basis of the (largest) moment of inertia of the trans-HOCO intermediate[13] (as employed previously by Casavecchia and co-workers[17,18] in their estimate of the rotational period of the HOCO complex formed during the reverse OH + CO reaction), an impact parameter $b \sim 1.5$ Å (cf. the equilibium bond length of CO in the reactant CO_2, $r_e = 1.2$ Å), equivalent to an orbital angular momentum $|L| \sim 45\hbar$, would generate a complex with a rotational period of ~1.0 ps. The observation of *backward* scattering suggests that rather lower impact parameter collisions are responsible for generating the OH($N' = 1$) products in question, and any intermediate complex formed is likely to rotate with an even longer period, $\tau_r > 1$ ps. Given, in addition, that the experimentally determined HOCO lifetimes are between 0.2[3,4] and 0.6 ps[6] at an excess energy of ~1.1 eV above the OH + CO asymptote, the highly anisotropic, backward scattering of OH($v' = 0$, $N' = 1$) at the *higher* excess energy $E \sim 1.4$ eV (i.e., a mean collision energy 2.5 eV) is not surprising. It is interesting to note that the preferential production of low rotational states of OH($v' = 0$) via low impact parameter collisions would also provide an attractive rationale for the enhanced population of low N' levels found by Wittig and co-workers[26] in their study of the photolysis of HBr bound to CO_2 in a van der Waals complex.

The above conclusions, regarding the OH($v' = 0$, $N' = 1$) products of the H + CO_2 reaction at a mean collision energy of 2.5 eV, are consistent with the *dynamical* interpretation of the scattering into the (more probable) OH($v' = 0$, $N' = 5$) + CO[11] channel at the same collision energy (see section 1 and Figure 5). Although it is attractive to associate the forward−backward peaking DCS in this channel with "long-lived" complex behavior, the dissociation and rotational time scales,

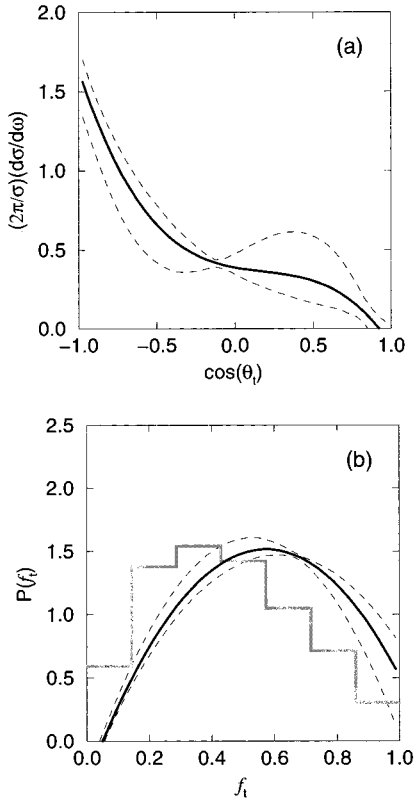

Figure 4. The OH($v' = 0$, $N' = 1$) angular distribution (a) and the distribution in the fractional energy release into translation $P(f_t)$ (b) from the H + CO_2 reaction at a collision energy of 2.5 eV. The center-of-mass scattering angle θ_t in the upper panel is that between the CM velocities of OH and the reactant H atom. The best fit results are shown as bold lines, while the 95% confidence limits, based on a Monte Carlo error analysis, are shown as dashed lines. Also shown in the lower panel as a thick gray line is the phase space predicted $P(f_t)$ distribution.

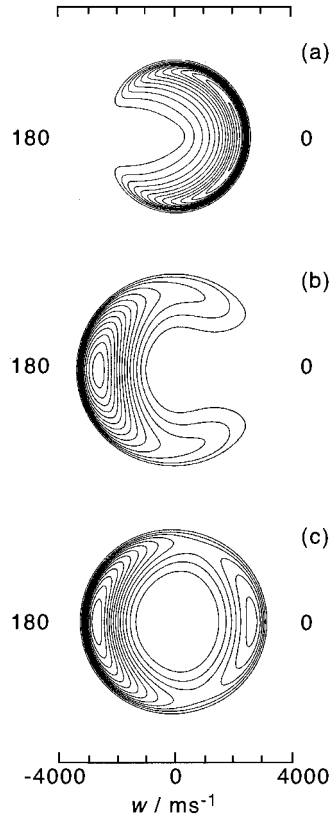

Figure 5. Polar scattering maps of the CM scattering angle-velocity distribution, $P(\theta_t, w)$, for the OH($v' = 0$, $N' = 1$) products of the H + CO_2 reaction at collision energies of 1.8 eV (a) and 2.5 eV (b). Panel c shows the polar map for the OH($v' = 0$, $N' = 5$, A') products of the reaction at the collision energy of 2.5 eV determined in reference 11.

based on the data currently available, are difficult to reconcile. Impact parameters in the range $b \geq 8-3$ Å would be required to bring the rotational period down to HOCO lifetimes in the range $\tau \leq 0.2-0.6$ ps (see above). These b values *exceed* the largest impact parameter employed in the trajectory calculations of Schatz and co-workers,[12] and seem unlikely to be involved based on current knowledge of the *ground* state PES.[12,13]

The measured HOCO dissociation times at the energy appropriate for complex formation from H + CO_2 at the *lower* collision energy (1.8 eV) range from 0.6[3,4,17,18] to 4.0 ps.[6] These time scales appear to be sufficiently long to allow significant rotation during the lifetime of the complex at these energies. Indeed, the change in OH($v' = 0$, $N' = 1$) angular distribution from slightly forward (1.8 eV) to strongly backward (2.5 eV) peaking might be taken to indicate the formation of a transitory collision complex which, at the lower collision energy, survives on average for half a rotational period (i.e., with $\tau_R \sim 1.2-8.0$ ps). Despite these longer time scales, dynamical factors (presumably exerted in the OH + CO exit channel of the reaction) still influence the CO coproduct internal energy disposals, although not as profoundly as those observed in the isoelectronic, but highly exothermic, H + N_2O reaction[21]).

The foregoing discussion assumes that all product channels are generated via reaction on the ground electronic potential energy surface. Although low-lying excited states are known to be accessible at the collision energies of the present experiments, particularly at HCO_2 configurations,[5] their role in the reaction is uncertain. Simple correlation arguments suggest that the ground electronic state of the reactants and the HOCO/HCO_2 intermediate correlates adiabatically with only one of the two spin−orbit states of the products OH($^2\Pi$) + CO($^1\Sigma$). Strong exit channel couplings between the ground and excited electronic surface would cloud this picture, and the involvement of higher electronic potential energy surfaces cannot be discounted at this stage. Future studies of the dependence of the angular and energy release distributions on OH spin−orbit state should clarify this point.[25]

5. Conclusions

Angular distributions and pair-correlated translational energy distributions have been measured for OH($v' = 0$, $N' = 1$), produced through the reactive scattering of H by CO_2 at 300 K and mean collision energies of 1.8 eV and 2.5 eV. The new measurements, together with those reported previously for the OH($v' = 0$, $N' = 5$, A'/A'') products of reaction at 2.5 eV, reveal that the differential cross sections depend sensitively on collision energy and product quantum state. Although less dramatic changes are evident in the pair-correlated kinetic energy release data, the measurements confirm that the pair-correlated CO internal energy distributions are considerably colder than those predicted by statistical phase space theory. The new results obtained at a collision energy of 2.5 eV support our previous findings that the product quantum state distributions, energy disposals, and angular distributions are primarily under dynamical control, while the results obtained at the collision energy of 1.8 eV are consistent with the intermediacy of a short-lived HOCO complex whose lifetime is comparable to its rotational period. The latter conclusions support those reached by Casavecchia and co-workers,[17,18] based on their study of the (state-averaged) angular distributions in the *reverse* OH + CO

reaction, at comparable total energies. Work currently in progress, to be reported elsewhere,[25] is exploring more fully the collision energy and OH (rovibrational and spin−orbit) state dependence of the reactive scattering unveiled in this interim report. However, it is already clear that the observation of highly anisotropic scattering in the present, state-resolved study of the $H + CO_2$ reaction at 2.5 eV, will provide a demanding test for ab initio theory.

Acknowledgment. We gratefully acknowledge Professor George Schatz for helpful discussions and for supplying us with an early copy of ref 12. We thank the EPSRC for a research grant and both the EPSRC and EC for providing postdoctoral support for K.S.K. Shell Research Ltd. is gratefully acknowledged for their funding of the studentship for D.W.H. Finally we thank Simon Gatenby for providing the program used in creating the polar plots shown in Figure 5.

References and Notes

(1) Fulle, D.; Hamann, H. F.; Hippler, H.; Troe, J. *J. Chem. Phys.* **1996**, *105*, 983.

(2) Kudla, K.; Schatz, G. C. In *Chemical Dynamics and Kinetics of Small Free Radicals*; Wagner, A., Liu, K., Eds.; World Scientific: Singapore, 1995; Part I, p 438.

(3) Ionov, S. I.; Brucker, G. A.; Jaques, C.; Valachovic, L.; Wittig, C. *J. Chem. Phys.* **1992**, *97*, 9486.

(4) Jaques, C.; Valachovic, L.; Ionov, S. I.; Bohmer, E.; Chen, Y.; Segall, J.; Wittig, C. *J. Chem. Soc., Faraday Trans.* **1993**, *89*, 1419.

(5) Kim, E. H.; Bradforth, S. E.; Arnold, D. W.; Metz, R. B.; Neumark, D. *J. Chem. Phys.* **1995**, *103*, 7801.

(6) Scherer, N. F.; Sipes, C.; Bernstein, R. B.; Zewail, A. H. *J. Chem. Phys.* **1990**, *92*, 5239.

(7) Rice, J. K.; Baronavski, A. P. *J. Chem. Phys.* **1991**, *94*, 1006.

(8) Jacobs, A.; Wahl, M.; Weller, R.; Wolfrum, J. *Chem. Phys. Lett.* **1989**, *158*, 161.

(9) Jacobs, A.; Volpp, H.-R.; Wolfrum, J. *Chem. Phys. Lett.* **1994**, *218*, 51.

(10) Nickolaisen, S. L.; Cartland, H. E.; Wittig, C. *J. Chem. Phys.* **1992**, *96*, 4378.

(11) Brouard, M.; Lambert, H. M.; Rayner, S. P.; Simons, J. P. *Mol. Phys.* **1996**, *89*, 403.

(12) Bradley, K. S.; Schatz, G. C.; *J. Chem. Phys.* **1997**, *106*, 8464.

(13) Schatz, G. C.; Fitzcharles, M. S.; Harding, L. B. *Faraday Discuss. Chem. Soc.* **1987**, *84*, 359.

(14) Clary, D. C.; Schatz, G. C. *J. Chem. Phys.* **1993**, *99*, 4578.

(15) Hernandez, M. I., Clary, D. C. *J. Chem. Phys.* **1994**, *101*, 2779.

(16) Bowman, J. M. *J. Phys. Chem.* **1998**, *102*, 3006 and references therein.

(17) Alagia, M.; Balucani, N.; Casavecchia, P.; Stranges, D.; Volpi, G. G. *J. Chem. Phys.* **1993**, *98*, 8341.

(18) Casavecchia, P.; Balucani, N.; Volpi, G. G. In *Chemical Dynamics and Kinetics of Small Free Radicals*; Wagner, A., Liu, K., Eds.; World Scientific: Singapore, 1995; Part I, p 365.

(19) Docker, M. P. *Chem. Phys.* **1989**, *135*, 405.

(20) Aoiz, F. J.; Brouard, M.; Enriquez, P. A. *J. Chem. Phys.*, **1996**, *105*, 4981.

(21) Brouard, M.; Burak, I.; Gatenby, S.; Markillie, G. A. J. *Chem. Phys. Lett.* **1998**, *287*, 682. Brouard, M.; Gatenby, S. In preparation.

(22) Ashfold, M. N. R.; Cook, P. A.; Langford, S. R.; Orr-Ewing, A. J.; Regan, P. M. *Proc. SPIE Conference* 1998, in press, and private communication.

(23) Chen, Y.; Hoffmann, G.; Oh, D.; Wittig, C. *Chem. Phys. Lett.* **1989**, *159*, 426.

(24) Alexander, A. J.; Blunt, D. A.; Brouard, M.; Simons, J. P.; Aoiz, F. J.; Bañares, L.; Fujimura, Y.; Tsubouchi, M. *Faraday Discuss. Chem. Soc.* **1997**, *108*, 375.

(25) Brouard, M.; Hughes, D. W.; Kalogerakis, K. S.; Simons, J. P. In preparation.

(26) Buelow, S.; Radhakrishnan, G.; Catanzarite, J.; Wittig, C. *J. Chem. Phys.* **1985**, *83*, 444. Radhakrishnan, G.; Buelow, S.; Wittig, C. *J. Chem. Phys.* **1986**, *84*, 727.